FUNDUS AUTOFLUORESCENCE LIFETIMES AND CENTRAL SEROUS CHORIORETINOPATHY

CHANTAL DYSLI, MD, LIESELOTTE BERGER, MD, SEBASTIAN WOLF, MD, PHD, MARTIN S. ZINKERNAGEL, MD, PHD

Purpose: To quantify retinal fluorescence lifetimes in patients with central serous chorioretinopathy (CSC) and to identify disease specific lifetime characteristics over the course of disease.

Methods: Forty-seven participants were included in this study. Patients with central serous chorioretinopathy were imaged with fundus photography, fundus autofluorescence, optical coherence tomography, and fluorescence lifetime imaging ophthalmoscopy (FLIO) and compared with age-matched controls. Retinal autofluorescence was excited using a 473-nm blue laser light and emitted fluorescence light was detected in 2 distinct wavelengths channels (498–560 nm and 560–720 nm). Clinical features, mean retinal autofluorescence lifetimes, autofluorescence intensity, and corresponding optical coherence tomography (OCT) images were further analyzed.

Results: Thirty-five central serous chorioretinopathy patients with a mean visual acuity of 78 ETDRS letters (range, 50–90; mean Snellen equivalent: 20/32) and 12 age-matched controls were included. In the acute stage of central serous chorioretinopathy, retinal fluorescence lifetimes were shortened by 15% and 17% in the respective wavelength channels. Multiple linear regression analysis showed that fluorescence lifetimes were significantly influenced by the disease duration ($P < 0.001$) and accumulation of photoreceptor outer segments ($P = 0.03$) but independent of the presence or absence of subretinal fluid. Prolonged central macular autofluorescence lifetimes, particularly in eyes with retinal pigment epithelial atrophy, were associated with poor visual acuity.

Conclusion: This study establishes that autofluorescence lifetime changes occurring in central serous chorioretinopathy exhibit explicit patterns which can be used to estimate perturbations of the outer retinal layers with a high degree of statistical significance.

RETINA 37:2151–2161, 2017

Central serous chorioretinopathy (CSC) is characterized by serous retinal detachment associated with leakage of fluid through the retinal pigment epithelium (RPE) into the subretinal space.[1] This disorder affects predominantly men with an average age range of 40 years to 51 years. There are numerous risk factors for the development of CSC discussed in literature. Best evidence is given for the association of CSC with the use of glucocorticosteroids.[1] In early phases of the disease, visual acuity may be normal. Later on, patients with CSC often report decreased and distorted vision associated with metamorphopsia, micropsia, dyschromatopsia, and reduced contrast sensitivity. The acute form of the disease is more often seen unilaterally in younger patients and generally resolves spontaneously with return to normal or almost normal visual acuity. Central serous chorioretinopathy can persist as a chronic form when the subretinal fluid remains over 3 months to 6 months. Recurrent forms of CSC are observed in over 50%.[2] Chronic CSC is associated with more severe and irreversible RPE damage that sometimes leads to permanent decrease in visual acuity. This disease stage is referred to as "diffuse retinal pigment epitheliopathy."[1]

Despite substantial research efforts in the last decades, the exact disease mechanism remains poorly understood. There are different theories of pathogenesis discussed, including the role of the choroid which is thought to be hyperpermeable, the role of the RPE with a loss of barrier and pumping function, and several other approaches like hormonal factors, and inflammatory and infectious disorders.[1]

Recent advances in different imaging modalities, such as optical coherence tomography (OCT), fundus autofluorescence (FAF) imaging, fluorescein angiography (FA), and indocyanine green angiography (ICGA), are helpful for diagnosis and disease documentation.[2]

Advanced technologies in fluorescence lifetime imaging microscopy (FLIM) have recently been described as useful tool to detect subtle variations in cellular metabolism in different metabolic conditions.[3] In analogy, fluorescence lifetime imaging ophthalmoscopy (FLIO) can be used to image lifetimes of endogenous retinal fluorophores on a macroscopic level.[4,5] In the FLIO technique, autofluorescence of the retina is excited with a laser impulse and the fluorescence lifetime represents the time the excited fluorophore spends in its higher energy level before returning to its basal level by releasing a long-wavelength photon.

In this study, we use FLIO to characterize and quantify retinal fluorescence lifetimes (FLT) using the mean lifetime (Tm) in CSC over the course of the disease.

Methods

Patients

Thirty-five patients with the clinical diagnosis of CSC and 12 age-matched healthy controls were included in this prospective study. This study was carried out with the approval of the local ethics committee and is in accordance with the International Ethical Guidelines for Biomedical Research involving Human Subjects (Council for International Organizations of Medical Sciences —CIOMS). It is registered at ClinicalTrials.gov (NCT01981148). All participants were recruited at the Department of Ophthalmology at the University Hospi-

Reprint requests: Martin S. Zinkernagel, MD, PhD, Bern University Hospital, 3010 Bern, Switzerland; e-mail: m.zinkernagel@gmail.com

tal of Bern and signed informed consent was required before study entry. Exclusion criteria for this study were age over 55 years, secondary choroidal neovascularization or other retinal diseases such as age-related macular degeneration, and choroidal neovascularization because of myopia that may cause subretinal fluid. Furthermore, patients with significant lens opacities that may interfere with the measurements were excluded.

Fluorescence Lifetime Imaging Ophthalmoscope

A fluorescence lifetime imaging ophthalmoscope (Heidelberg Engineering, Heidelberg, Germany) was used for acquisition of FLT measurements in the retina. The basic characteristics of the FLIO device and the analysis method have been described elsewhere in further detail.[4] Retinal fluorescence was excited using a 473-nm pulsed blue laser light at 80 MHz repetition rate.

The laser safety calculations have been provided by Heidelberg Engineering and were done according to the International Electrotechnical Commission (IEC) 60825-1:2007.[6] The safety specifications have previously been published in detail.[7] The scanning beam within the FLIO system is below Class I accessible emission limits. For registration of emitted fluorescence light by time-correlated single-photon counting (TCSPC) modules, highly sensitive hybrid photon-counting detectors (Becker&Hickl, Berlin, Germany) were used. Emitted fluorescence photons were measured in 2 separate wavelength ranges: a short spectral channel (SSC: 498–560 nm) and a long spectral channel (LSC: 560–720 nm). A minimum of 1,000 photons per pixel was acquired in both channels, which required a mean scan duration of approximately 90 seconds per eye. To detect each photon at the correct spatial location, a high-contrast confocal infrared image was simultaneously recorded. Analysis of lifetime data was performed by the Becker&Hickl software (SPCImage 4.6), which allowed calculating a mean lifetime value for each pixel. A binning factor of one with a biexponential fitting algorithm was used. The goodness of the exponential fit was assessed by the chi-square value.

The mean lifetime value Tm was calculated from a short (T1) and a long (T2) lifetime component with their corresponding amplitudes (relative contribution) $\alpha1$ and $\alpha2$ using the following equation:

$$Tm = \frac{\alpha1 \times T1 + \alpha2 \times T2}{\alpha1 + \alpha2} \qquad (1)$$

Image Acquisition

All patients had a complete dilated eye exam before image acquisition. Best-corrected visual acuity was
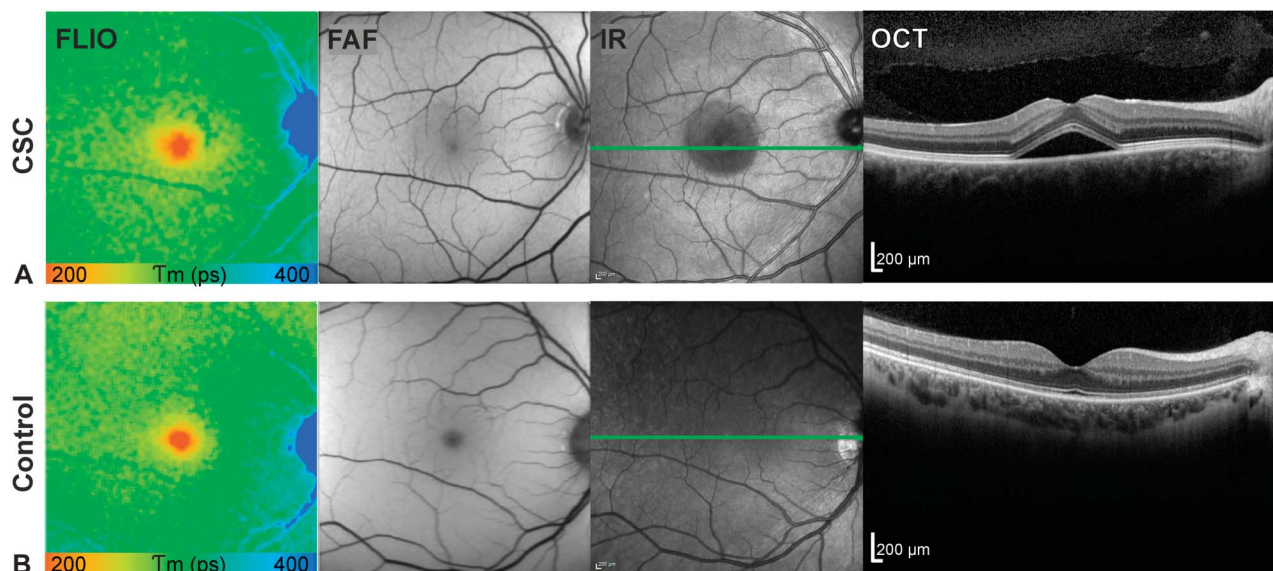
Fig. 1. Fluorescence lifetime imaging in CSC with recent disease onset. **A.** Acute CSC with 3 days duration of symptoms (33-year-old male patient). Subretinal fluid is evident in OCT; however, mean FLT are comparable to controls. **B.** Healthy control subject. Corresponding fluorescence lifetime image (FLIO) of the long spectral channel (560–720 nm, color scale: 200–400 ps), FAF, and IR image where the location of the OCT scan is shown as green line.

assessed for every participant (BCVA shown in Early Treatment Diabetic Retinopathy Study [ETDRS] letters[8] and Snellen equivalent). The diagnosis of CSC was based on fundus examination, OCT, fluorescein angiography, and indocyanine green angiography. The presumed onset of CSC was determined from patients' history of blurred or decreased vision, dyschromatopsia, micropsia, or metamorphopsia. Fluorescence lifetime images were acquired from both eyes from every participant using a fluorescence lifetime imaging ophthalmoscope. Additionally, fundus color images (Zeiss FF 450plus; Zeiss, Oberkochen, Germany) and OCT scans of the macula (Spectralis HRA +OCT; Heidelberg Engineering) were obtained as part of their general ophthalmic examination and disease documentation.

Nineteen patients were examined repeatedly. For analysis, data from only one eye per patient was used. To assess FLT changes according to disease duration, patients were divided into 3 groups according to the disease duration: less than 6 months, 6 months to 18 months, and over 18 months.

Fluorescence Lifetime Measurement in Retinal Pigment Epithelium Cell Cultures

To quantify autofluorescence lifetime of pure RPE, FLIO measurement of RPE cell cultures in vitro was performed. Therefore, human RPE cells were cultured within culture medium (DMEM + GlutaMAX + 10% FCS + 1% AA; Gibco, Thermo Fisher Scientific, Waltham, MA) in glass chamber slides at 37°C and

5% CO_2 for 4 days until a cell count of ca. 30,000 cells was reached yielding a confluent monolayer. Before FLIO measurement, the culturing solution was removed and cells were covered with PBS solution. In a second step, *all-trans* retinal solution (1 mg/mL; Sigma-Aldrich, Buchs, Switzerland) was applied on the RPE cells and FLIO was measured again.

Statistical Analysis

A standard early treatment of diabetic retinopathy (ETDRS) grid was used to average FLT within each grid sector (FLIO reader, ARTORG Center for Biomedical Engineering Research, University of Bern, Switzerland). Mean lifetime values of the central area (C, diameter (d) = 1 mm), the inner ring (IR, d = 3 mm), and the outer ring (OR, d = 6 mm) were used for further analysis.

Statistical analysis was performed using Prism Graph Pad (Prism 6; GraphPad Software Inc, La Jolla, CA). Affected retinal areas in eyes with CSC in different disease stages were compared with corresponding age-matched healthy control eyes by one-way ANOVA and Tukey's multiple comparison posttest analysis (confidence interval 95%). A linear regression model was used for correlation analysis. *P* values of less than 0.05 were considered to be statistically significant. Fluorescence lifetime data of both spectral channels were analyzed separately. Multiple linear regression analysis was done using SigmaPlot version 12.3 (Systat Software Inc, San Jose, CA).
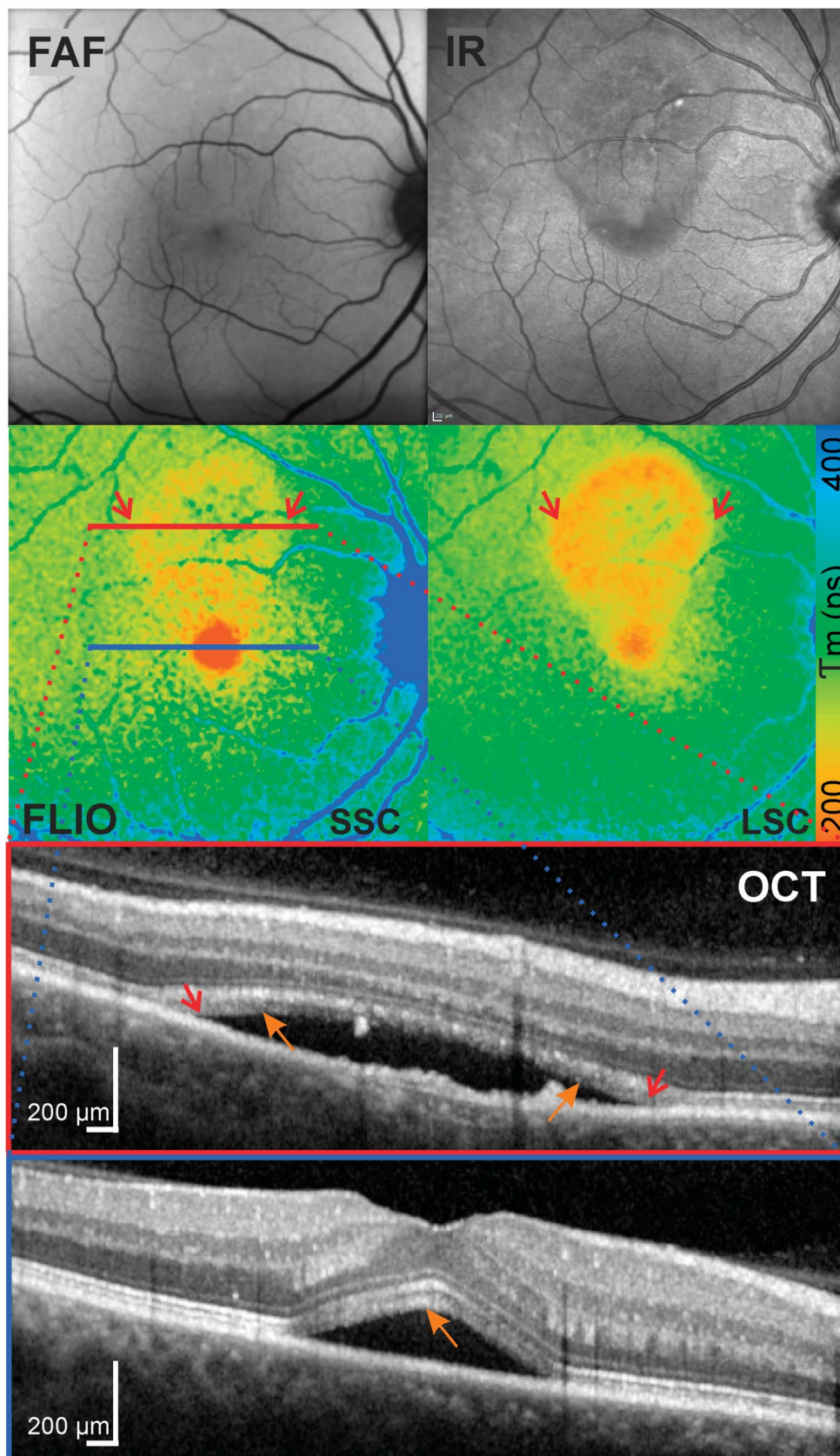
Fig. 2. Fluorescence lifetime imaging in CSC. Right eye of a 50-year-old male patient with CSC disease duration of 3 months. Color-coded fluorescence lifetime images in the short (SSC: 498–560 nm) and the long (LSC: 560–720 nm) spectral channel (color range: 200–400 ps). The red and blue bars represent the OCT scan line of the OCT scans below. Red arrows delineate the retinal area with subretinal fluid and elongated outer photoreceptor segments represented by short mean fluorescence lifetimes in both the short and long spectral lifetime channel. Corresponding accumulation of photoreceptor outer segments is marked in the OCT (orange arrows). FAF, fundus autofluorescence; IR, infrared image.
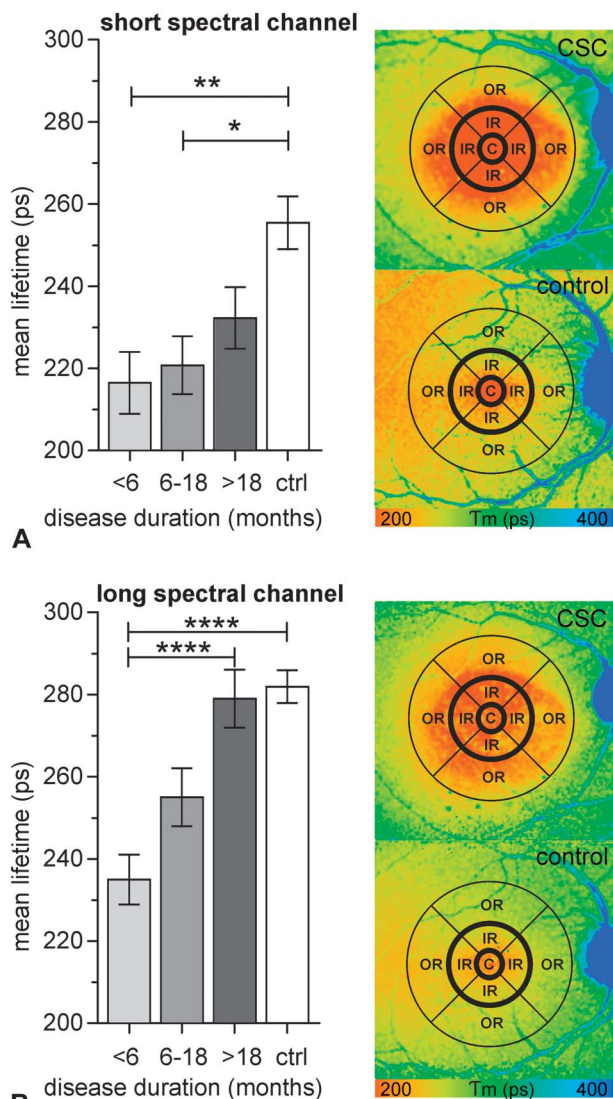
Fig. 3. Quantitative analysis of fluorescence lifetimes in CSC. Bar graphs showing mean values for the inner ETDRS ring (IR) of the short (**A**, 498–560 nm) and the long (**B**, 560–720 nm) spectral channel with corresponding representative FLIO images of a 44-year-old female patient with disease duration of 6 months. Data were assigned to 3 groups depending on the duration of disease (<6 months, between 6 and 18 months, and >18 months) (mean ± SEM; ps = picoseconds; one-way ANOVA and Tukey's multiple comparison posttest analysis; *$P <$ 0.05, **$P <$ 0.01, ****$P <$ 0.0001; n = 15, 11, 16, and 12 per group; color scale: 200–400 ps).

Results

Data of 35 eyes with central serous chorioretinopathy of 35 patients and 12 age-matched control subjects were analyzed in this study. All participants were phakic. Mean age (±Standard deviation) in the CSC group was 46.11 (±6.34, range, 29–53) years and 46.08 (±8.15, range, 37–55) years in the control group ($P =$ 0.99). The mean disease duration at time of the first FLIO measurement was 24.4 ± 5.3 (SEM) months (range:

0–120 months). None of the patients had secondary choroidal neovascularization as assessed by fluorescein angiography. Fifteen patients were investigated in the acute disease stage (0–6 months), 11 between 7 and 18 months, and 16 after over 18 months reported disease duration. Nineteen patients were investigated repeatedly at different stages of disease (duration of follow-up: mean, 9.5 months; range, 2–20 months).

Fluorescence Lifetimes in the Acute Disease Stage of Central Serous Chorioretinopathy

In patients with acute CSC with reported symptoms of only few days, neither autofluorescence intensity nor FLT did show any disease specific signs and were comparable to FLIO of age-matched healthy control eyes (Figure 1). In this very early disease stage, characteristic subretinal fluid accumulation was clearly identifiable in the optical coherence tomography and the infrared (IR) image. However, there was no sign of changes within the outer segments of the photoreceptors or the RPE. With longer duration of the disease, retinal areas of current or previous retinal detachment because of subretinal fluid accumulation in acute CSC were characterized by significantly shorter mean FLT in both spectral channels (Figure 2). In the inner ring of the ETDRS grid, mean lifetime values Tm were 216 ± 8 ps (SEM) in the short and 235 ± 6 ps in the long spectral channel. Thereby, Tm was shortened by 15% in the short and by 17% in the long spectral channel compared to healthy control eyes ($P <$ 0.01 and $P <$ 0.0001, respectively; Figure 3). A similar reduction in FLTs in the long spectral channel was also seen in the outer ETDRS ring ($P =$ ns and $P <$ 0.001, respectively) and in the central subfield ($P =$ ns and $P <$ 0.0001). In normal conditions, mean FLT have been shown to be shortest within the macular center,[4] probably because of macular pigment.[9]

Correlation of Fluorescence Lifetime With Fluorescein Angiography Findings

In seven patients with recent onset of CSC, a leakage point was identified in fluorescein angiography. The leakage source was identifiable with distinctly longer FLT in 5 out of these 7 patients (Figure 4 and see **Figure 1, Supplemental Digital Content 1**, http://links.lww.com/IAE/A561).

Subretinal Fluid and Fluorescence Lifetimes

In a subgroup of 8 patients with acute CSC, FLT maps were compared when subretinal fluid was present and when it was reabsorbed (Figure 4, A and B). We did not find any differences in mean
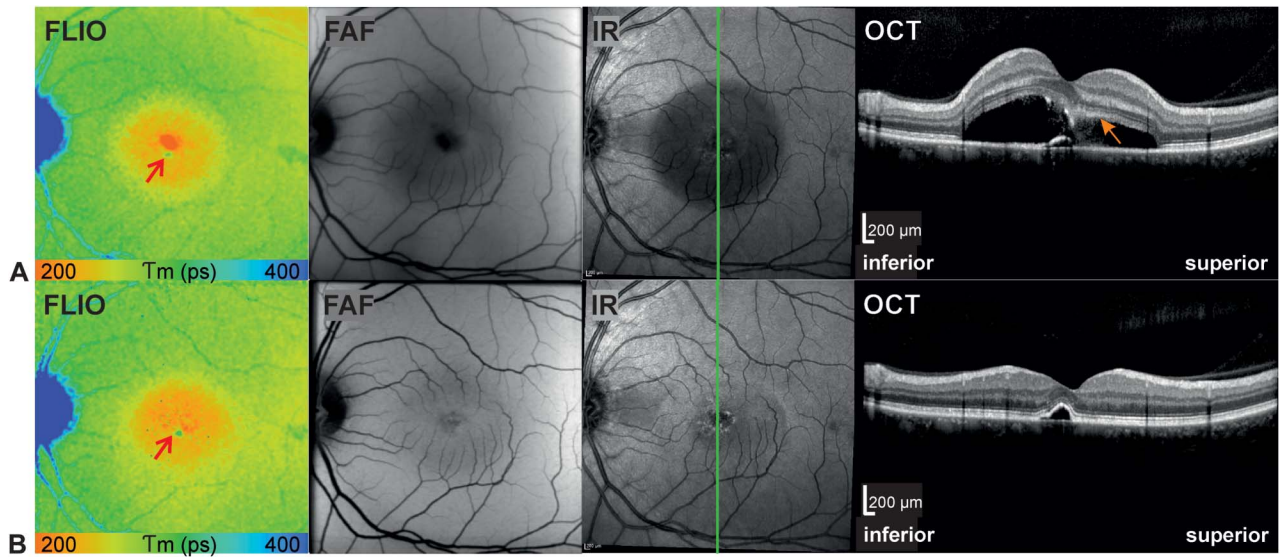
Fig. 4. Influence of subretinal fluid on fluorescence lifetimes (FLT). **A** and **B.** Subretinal fluid in chronic recurrent CSC of the affected left eye of a 45-year-old male patient with disease duration of 15 (with subretinal fluid, A) and 17 months (without fluid, B). The area with long mean FLT (red arrow) represents the leakage point in fluorescein angiography (see **Figure 1, Supplemental Digital Content 1**, http://links.lww.com/IAE/A561). Accumulation of photoreceptor outer segments is marked in the OCT (orange arrow). Corresponding fluorescence lifetime image (FLIO) of the long spectral channel (560–720 nm, color scale: 200–400 ps), FAF, and IR image where the location of the OCT scan is shown as green line.

FLT values between these 2 conditions (SSC: $P = 0.9$; LSC: $P = 0.2$).

In cases with subretinal fluid (n = 19), accumulation of photoreceptor outer segments measured in OCT correlated with short mean FLT of the long spectral channel ($r^2 = 0.18$; $P = 0.02$; see orange arrows in OCTs of Figures 2, 4, and 5).

Visual Acuity

The mean visual acuity at time of FLIO measurement was 78 ± 1 (SEM) ETDRS letters (range: 50–90; mean Snellen equivalent: 20/32). Assessed over all measurements, shorter mean FLT within the macular center were associated with better visual acuity in both spectral channels ($P = 0.13$ and 0.17 respectively). This tendency was most pronounced in patients with disease duration >18 months.

Multiple Linear Regression Analysis

We analyzed the influence of the independent variables patient's age, disease duration, visual acuity, and presence/absence of subretinal fluid on the mean fluorescence lifetime (central ETDRS subfield, SSC resp. LSC) as the dependent variable. In the SSC, the patient's age did significantly contributed to the ability to predict the dependent variable mean FLT Tm ($P = 0.03$). In the LSC, Tm was significantly influenced by the disease duration ($P < 0.001$) but independent of the presence or absence of subretinal fluid ($P = 0.4$). In the presence of subretinal fluid, short mean FLT were correlated with accumulation of photoreceptor outer segments ($P = 0.03$).

When analyzing the influence of the independent variables patient's age and disease duration on Tm of the inner ETDRS ring, increasing age was significantly correlated with longer mean FLT in both channels (SSC: $P = 0.003$ and LSC: $P = 0.006$). In the LSC, short disease duration was significant associated with shorter mean FLT (<0.001).

Autofluorescence Lifetimes Secondary to Retinal Changes in Chronic Central Serous Chorioretinopathy

In chronic disease stages, fluid accumulation and subsequent retinal changes followed the gravity and extended into the inferior part of the retina. In this stage, a mixed pattern of chorioretinal changes was observed (Figures 5 and 6). In OCT, drusenoid retinal deposits, retinal scars, and subsequent atrophy were identifiable. These changes were generally characterized by prolonged mean FLT in FLIO measurements (SSC: +112 ps = 367 ± 20 ps, LSC: +123 ps = 405 ± 20 ps; Figure 6B).

Analysis of Individual Fluorescence Lifetime Components

Because Tm represents the intensity weighted mean FLT (see Equation 1), individual lifetime components of Tm were further analyzed in detail. Distribution histograms of the short decay component (T1) plotted
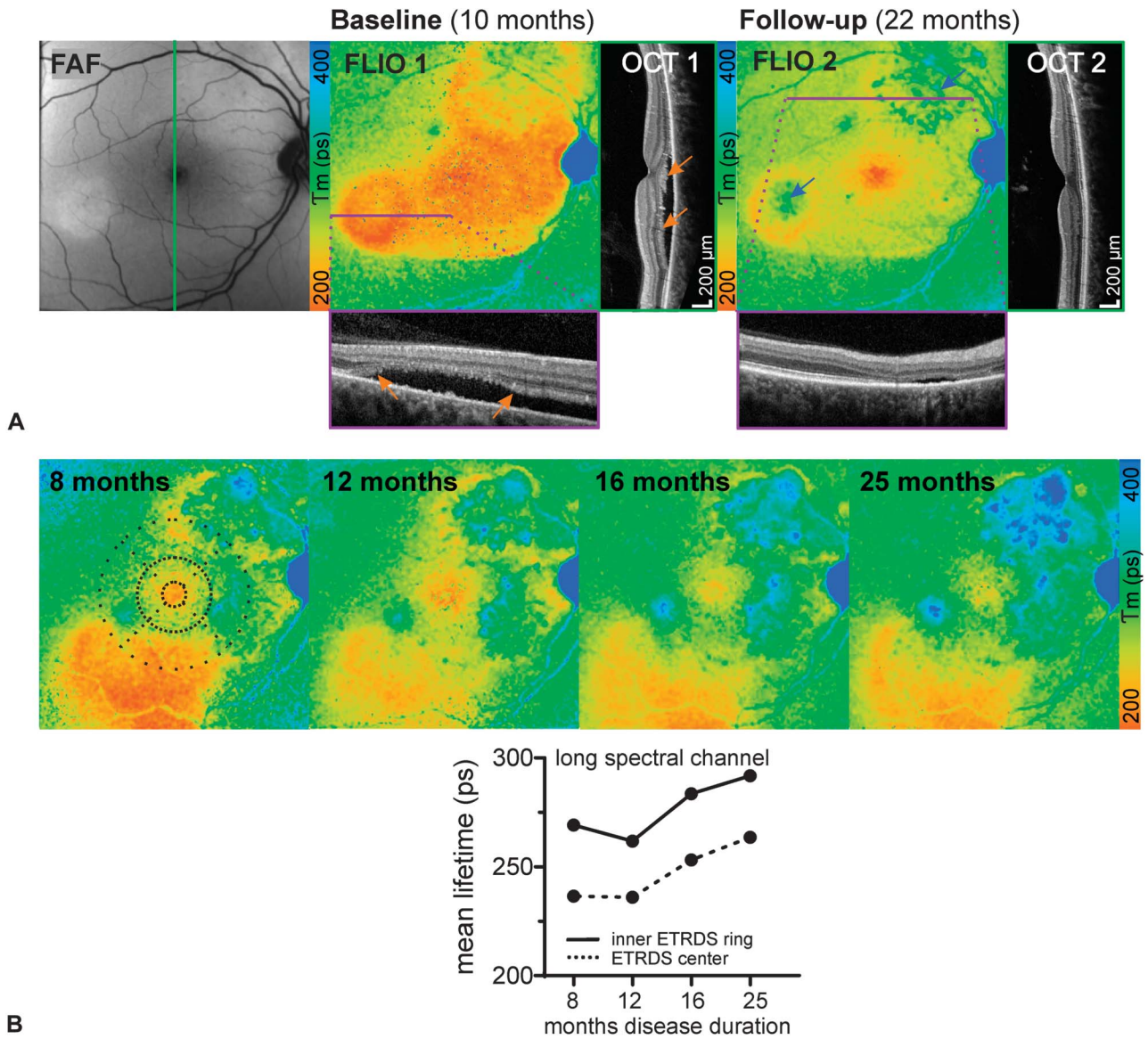
Fig. 5. Fluorescence lifetime (FLIO) changes in CSC over the course of time. **A.** One-year follow-up of CSC at 10 months (FLIO 1 and OCT 1) and 22 months (FLIO 2 and OCT 2) after disease onset (51-year-old male patient). Accumulation of photoreceptor outer segments is marked in the OCT (orange arrows). Prolonged lifetimes are identified in areas where retinal atrophy developed (blue arrows). Fluorescence lifetime images (FLIO) of the long (LSC: 560–720 nm) spectral channel (color scale: 200–400 ps), FAF, and OCT scans (scan location is shown in the FAF [vertical scans] and FLIO [horizontal scans] images). **B.** Development of chronic CSC in FLIO over 17 months with quantification of mean FLT of the central and the inner ETDRS ring (diagram).

against the long decay component (T2) of eyes with CSC were compared with histograms of healthy control eyes (Figure 7A). Different anatomical regions showed specific dot plot distribution in the T1-T2 histogram.

The fovea featured the shortest FLT components in T1 as well as T2, and was clearly discernible as an individual lifetime cloud in the dot plot. The retinal vessels displayed long T2 lifetimes, whereas the optic nerve head showed long T1 and T2 lifetimes. The main retina featured T1 decay times in a narrow spectrum between 150 and 200 ps in the short spectral channel with a broad range in T2 (1,500–3,000 ps) and represented a well-distinguishable lifetime cloud in the dot plot graph.

In case of CSC, an additional FLT cloud adjacent to the retina was identifiable with shorter T1, contributing to a shorter mean FLT Tm (Figure 7A).

Additionally, the short and the long lifetime components were individually shown weighted with their respective amplitudes $\alpha 1$ and $\alpha 2$. Here as well, the foveal center, the optic nerve head, retinal vessels,
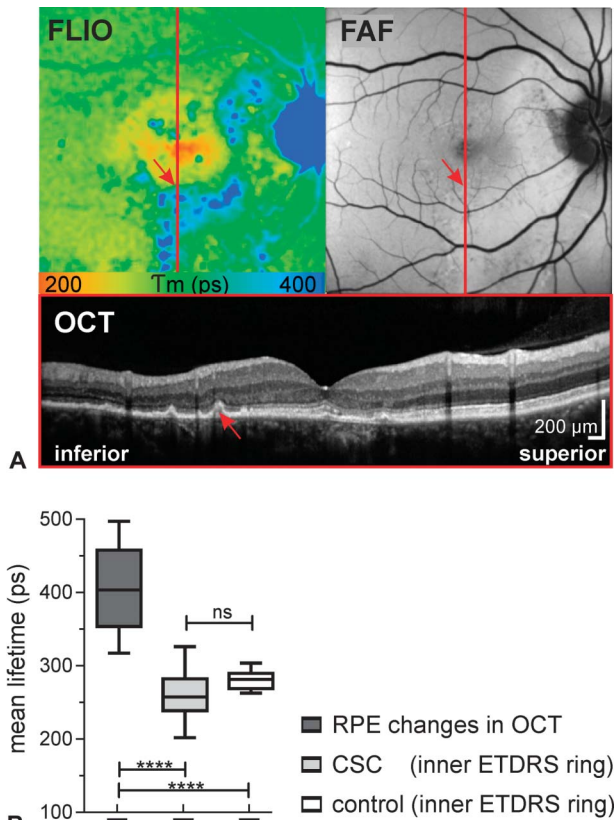
Fig. 6. Lifetime analysis of retinal pigment epithelium changes in chronic CSC. **A.** Right eye with CSC disease duration of 120 months (46-year-old male patient). Fluorescence lifetime images (FLIO) of the long (LSC: 560–720 nm) spectral channel (color scale: 200–400 ps), FAF, and OCT scans with scan location indicated by the red line in the FAF and FLIO images. Secondary changes of the RPE and the retinal architecture are evident in OCT. Arrows highlight corresponding areas in FAF, FLIO, and OCT with prolonged lifetimes. **B.** Quantification of fluorescence lifetimes in the LSC within the inner ETDRS ring in areas with RPE changes as seen by OCT (n = 9), in areas with CSC (n = 35), and in healthy controls (n = 12) (Box: median ± 25%, whiskers: min–max; ps = picoseconds; one-way ANOVA and Tukey's multiple comparison posttest analysis; *$P < 0.05$, ****$P < 0.0001$, ns = not significant).

the peripheral retina, and the area of CSC were clearly identifiable (Figure 7B).

Fluorescence Lifetime Measurement in Retinal Pigment Epithelium Cell Cultures

Fluorescence lifetime imaging ophthalmoscopy of in vitro RPE cells revealed weak autofluorescence intensity because of the absence of lipofuscin and mean autofluorescence lifetimes of 1,670 ps in the short and 1,250 ps in the long spectral channel. In pure *all-trans* retinal, Tm was 50 and 40 ps, respectively. The combination of RPE cells with *all-trans* retinal solution revealed mean FLT of 120 and 63 ps, respectively (see **Figure 2, Supplemental Digital Content 2**, http://links.lww.com/IAE/A562). When analyzing this

data in the 2D distribution histogram, each measurement condition was discernible with a characteristic T1-T2 distribution. However, in the RPE-retinal combination, only one dot plot, independent of the 2 components, was identified (see **Figure 2D, Supplemental Digital Content 2**, http://links.lww.com/IAE/A562). This shows that the inferred FLT represent a bulk response from many individual lifetime components.

Discussion

In this study, we analyzed lifetime maps of endogenous retinal fluorophores in 35 patients with CSC and compared them with age-matched healthy controls. In the acute stage of CSC, we identified an area of shorter retinal FLT corresponding to the area of serous retinal detachment. With time, the occurrence of short autofluorescence lifetimes decreased. Former borders of chorioretinal changes often remained visible. In chronic disease stages, areas with secondary changes of the retina and the RPE were characterized by prolonged mean retinal FLT. Furthermore, in approximately 70%, the leakage point in fluorescein angiography was identifiable by distinctly longer FLT in FLIO.

Even though the pathophysiology of CSC is not entirely clarified, the latest consensus for disease mechanism and development is a hyperpermeability of the choroid. Increased hydrostatic pressure results in fluid accumulation and fibrin leakage into Bruch membrane within the subretinal space.[1] Additionally, the retinal pigment epithelium loses its barrier and pumping function, which further aggravates the imbalance between fluid formation and resorption. Several studies have shown that previous or chronic subretinal fluid leads to increased autofluorescence intensity.[10,11] Increased autofluorescence intensity is mainly thought to originate from by-products of the visual cycle, in general from lipofuscin and its derivates.[12] According to our study, FLT were shortened in the acute stage even when subretinal fluid was absent. Hence, neither the fluid components nor the shorter distance of the sensor to the detached retina seems to have an impact on FLT. However, there were considerable differences in lifetime measurements with different disease durations. While immediately after onset of fluid accumulation no difference in lifetimes was measured, within the first weeks, a shift toward short FLT was observed. As the measured mean FLT represents a bulk of signals that combines short and long decay times, changes in the equilibrium of different fluorophores will result in altered autofluorescence lifetimes. The FLT measured in the acute disease
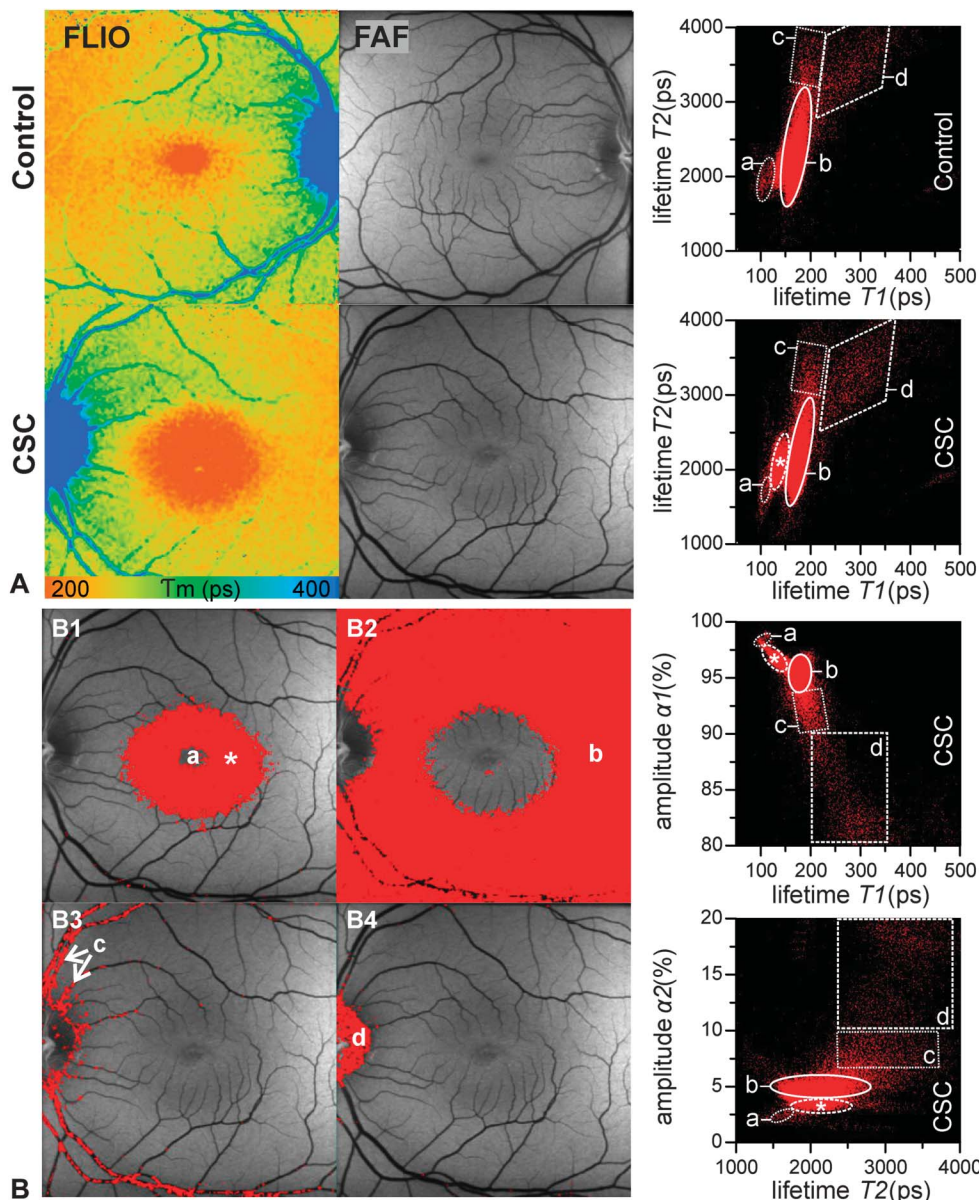
Fig. 7. Analysis of individual lifetime components and spatial distribution in CSC. **A.** Fluorescence lifetime images (FLIO, short spectral channel) and corresponding autofluorescence intensity images (FAF) of the right healthy fellow eye *(upper row)* and the left eye with CSC *(lower row)* (color scale: 200–400 ps) in a 44-year-old patient with disease duration of 15 months. Corresponding distribution histograms of the short decay component T1 versus the long decay component T2 (see also Equation 1) are shown (right panel). Spatial distribution of different lifetime clusters: a) macular center, b) neurosensory retina, c) retinal vessels, d) optic nerve head, and *) area of CSC. **B.** Distribution of the lifetime cluster areas shown in the histograms in B: (**B1**) Area of CSC, (**B2**) neurosensory retina, (**B3**) retinal vessels, (**B4**) optic nerve head. Distribution histograms of the short decay component T1 versus the corresponding amplitude α1 *(above)* and the long decay component T2 versus the corresponding amplitude α2 *(below)* are shown beside with specific distribution clusters as described in **A**.

stage may derive from accumulation of intermediate components of the visual cycle with very short mean autofluorescence lifetime values.[13] We found a correlation between the accumulation of the outer photoreceptor segments and the mean FLT, potentially indicating the cluster of visual cycle derivates. A recent paper from Sparrow et al[14] suggests that retinoid cycle by-products accumulate within outer segments of photoreceptor cells in Stargardt disease where there is dysfunction of the visual cycle.

Rhodopsin photoactivation leads to the isomerization of *11-cis* retinal to *all-trans* retinal. *All-trans* retinal has been shown to accumulate in the outer segments of the photoreceptors when phagocytosis

by the RPE is impaired.[15] *All-trans* retinal is released into the photoreceptor disk membrane and is covalently bound to the amine group of phosphatidylethanolamine (PE), forming N-retinylidene-PE (NRPE).[16] N-retinylidene-PE is then converted to N-retinylidene-N-retinyl-phosphatidylethanolamine (A2PE)[17] which in turn is a precursor of N-retinylidene-N-retinylethanolamine (A2E). All of these precursors are autofluorescent and form in the outer segments before phagocytosis by the RPE[18,19] and therefore will influence FLT within the CSC-affected area. As such, not only an underlying dysfunction of the RPE, which leads to accumulation of lipofuscin within the RPE itself, but the inability of the outer photoreceptor segments to release its products

of the phototransduction cycle[11] is likely to contribute to increased autofluorescence intensity and altered autofluorescence lifetimes.

To differentiate FLT components of the retina, ex vivo measurements of RPE cells and *all-trans* retinal were performed. Retinal pigment epithelium cells in vitro displayed quite long average mean FLT of 1,670 ps in the SSC and 1,250 ps in the LSC. However, *all-trans* retinal in an ethanol solution exhibited very short average FLT of 50 ps in the short and 40 ps in the long spectral channel. When adding *all-trans* retinal solution (diluted) onto the RPE single cell layer, FLT were considerably reduced with 120 and 63 ps compared with the RPE alone. These findings suggest that average FLTs in the human retina may be reduced by short FLT from components of the retinoid cycle during the acute disease stage. In the chronic stages of CSC, increased concentrations of lipofuscin are likely to tip the balance toward longer FLT as lipofuscin ex vivo has been shown to exhibit long FLT of 367 ps in the SSC and 405 ps in the LSC compared with surrounding retinal structures.[20]

Fluorescence lifetime imaging has several advantages over conventional fundus autofluorescence imaging. Time-resolved autofluorescence provides absolute values of FLTs, thereby allowing quantification of changes occurring during the course of CSC. In contrast to conventional fundus autofluorescence which offers a mean to assess integrity of the retinal pigment epithelium, fluorescence lifetime imaging can provide information about the integrity of the photoreceptors. Another potential advantage, which we did not further investigate in this study, is that fluorescence lifetime imaging can be used to assess macular pigment.[9,21] A recent study has shown a correlation between macular pigment optical density and CSC duration.[22] Because FLT are specific for each fluorophore and independent of their concentration, individual components of the visual cycle can be analyzed and characterized ex vivo. As such, autofluorescence lifetime imaging provides quantitative spatial information on metabolic retinal diseases and may be more suited to guide treatment decisions than conventional fundus autofluorescence.

Caution is needed when extrapolating observations from ex vivo measurements into in vivo conditions in the human retina, as the FLT signal in vivo derives from various endogenous fluorophores. Therefore, proof of the concept that *all-trans* retinal is potentially contained in unphagocytized outer segments or released into the subretinal space may account for part of the decreased autofluorescence lifetimes in CSC needs to be confirmed in a suitable animal model of chronic serous retinal detachment. This quest may be facilitated by the possibility to obtain information on individual lifetime components such as T1, T2 and the corresponding amplitudes by 2-dimensional plotting of individual lifetime clusters as seen in **Supplemental Digital Content 2** (see **Figure 2**, http://links.lww.com/IAE/A562). Individual components of the visual cycle can be analyzed ex vivo and findings can be translated into data obtained from in vivo measurements.

Given the high percentage of spontaneous resolution of CSC, the question arises whether FLT may be suited to monitor disease and to guide the timing of treatment such as photodynamic therapy. Fluorescence lifetimes may give a clue of the functional state of the photoreceptors as short lifetimes may suggest that the phototransduction cycle is still intact. Appearance of longer lifetimes may suggest structural damage and therefore may represent an indication to initiate treatment. However, larger prospective studies will be needed to address these questions adequately.

Conclusion

Retinal changes after central serous chorioretinopathy can be monitored by the measurement of FLT of retinal fluorophores. In the acute disease stage, CSC is characterized by an increased area of short lifetimes in the macular center, whereas retinal changes in chronic CSC are associated with prolonged autofluorescence lifetimes.

Fluorescence lifetime imaging might be used as a diagnostic tool for noninvasive monitoring of disease activity and metabolic changes within the retina in CSC.

Key words: CSC, CSCR, CSR, FLIO, fluorescence lifetimes, fundus autofluorescence, ophthalmic imaging, serous chorioretinopathy.

References

1. Nicholson B, Noble J, Forooghian F, Meyerle C. Central serous chorioretinopathy: update on pathophysiology and treatment. Surv Ophthalmol 2013;58:103–126.
2. Liegl R, Ulbig MW. Central serous chorioretinopathy. Ophthalmologica 2014;232:65–76.
3. Becker W. Fluorescence lifetime imaging—techniques and applications. J Microsc 2012;247:119–136.

4. Dysli C, Quellec G, Abegg M, et al. Quantitative analysis of fluorescence lifetime measurements of the macula using the fluorescence lifetime imaging ophthalmoscope in healthy subjects. Invest Ophthalmol Vis Sci 2014;55:2106–2113.

5. Dysli C, Wolf S, Zinkernagel MS. Fluorescence lifetime imaging in retinal artery occlusion. Invest Ophthalmol Vis Sci 2015;56:3329–3336.

6. International Electrotechnical Commission (IEC). International Standard 60825-1:2007 (Edition 2, ISBN 2-8318-9085-3)/60825-1:2014 (Edition 3, ISBN 978-2-8322-1499-2). International Electrotechnical Commission, TC 76, ICS 13.110, ICS 31.260.

7. Dysli C, Wolf S, Hatz K, Zinkernagel MS. Fluorescence lifetime imaging in Stargardt disease: potential marker for disease progression. Invest Ophthalmol Vis Sci 2016;57:832–841.

8. Early Treatment Diabetic Retinopathy Study design and baseline patient characteristics. ETDRS report number 7. Ophthalmology 1991;98:741–756.

9. Sauer L, Schweitzer D, Ramm L, et al. Impact of macular pigment on fundus autofluorescence lifetimes. Invest Ophthalmol Vis Sci 2015;56:4668–4679.

10. Matsumoto H, Kishi S, Sato T, Mukai R. Fundus autofluorescence of elongated photoreceptor outer segments in central serous chorioretinopathy. Am J Ophthalmol 2011;151:617–623.e1.

11. Spaide RF, Klancnik JM Jr. Fundus autofluorescence and central serous chorioretinopathy. Ophthalmology 2005;112:825–833.

12. Delori FC, Dorey CK, Staurenghi G, et al. In vivo fluorescence of the ocular fundus exhibits retinal pigment epithelium lipofuscin characteristics. Invest Ophthalmol Vis Sci 1995;36:718–729.

13. Loguinova MY, Zagidullin VE, Feldman TB, et al. Spectral characteristics of fluorophores formed via interaction between all-trans-retinal with rhodopsin and lipids in photoreceptor membrane of retina rod outer segments. Biochem (Mosc) Suppl Ser A: Membr Cell Biol 2009;3:134–143.

14. Sparrow JR, Marsiglia M, Allikmets R, et al. Flecks in recessive Stargardt disease: short-wavelength autofluorescence, near-infrared autofluorescence, and optical coherence tomography. Invest Ophthalmol Vis Sci 2015;56:5029–5039.

15. Maeda T, Golczak M, Maeda A. Retinal photodamage mediated by all-trans-retinal. Photochem Photobiol 2012;88:1309–1319.

16. Ebrey T, Koutalos Y. Vertebrate photoreceptors. Prog Retin Eye Res 2001;20:49–94.

17. Ben-Shabat S, Parish CA, Vollmer HR, et al. Biosynthetic studies of A2E, a major fluorophore of retinal pigment epithelial lipofuscin. J Biol Chem 2002;277:7183–7190.

18. Liu J, Itagaki Y, Ben-Shabat S, et al. The biosynthesis of A2E, a fluorophore of aging retina, involves the formation of the precursor, A2-PE, in the photoreceptor outer segment membrane. J Biol Chem 2000;275:29354–29360.

19. Fishkin N, Jang YP, Itagaki Y, et al. A2-rhodopsin: a new fluorophore isolated from photoreceptor outer segments. Org Biomol Chem 2003;1:1101–1105.

20. Schweitzer D, Gaillard ER, Dillon J, et al. Time-resolved autofluorescence imaging of human donor retina tissue from donors with significant extramacular drusen. Invest Ophthalmol Vis Sci 2012;53:3376–3386.

21. Dysli C, Wolf S, Zinkernagel MS. Autofluorescence lifetimes in geographic atrophy in patients with age-related macular degeneration. Invest Ophthalmol Vis Sci 2016;57:2479–2487.

22. Sasamoto Y, Gomi F, Sawa M, et al. Macular pigment optical density in central serous chorioretinopathy. Invest Ophthalmol Vis Sci 2010;51:5219–5225.